CORE
Metadata, citation and similar papers at core.ac.uk
Provided by Digital.CSIC

Ocean bottom pressure variability in the Mediterranean Sea and its relationship with sea level from a numerical model

Marta Marcos

IMEDEA (UIB-CSIC), C/Miquel Marquès, 21, 07190 Esporles, Spain

Tel.: +34 971611337 Fax: +34 971611761

marta.marcos@uib.es

The spatial and temporal scales of variability of ocean bottom pressure (P_b) in the Mediterranean Sea are characterized and their relationship with sea level assessed using a high resolution eddy-permitting regional ocean model spanning the period 1999-2011. It was found that rapid (periods of a few days) bottom pressure fluctuations are coherent with sea level and are decoupled between the eastern and western basins as a result of topographic constraints. In the longer periods, steric processes gained relevance away from the coast and partially broke the coherence between sea level and P_b, especially on the western basin. Results confirm that sea level changes are predominantly barotropic over most of the basin and at all time scales, except for the annual cycle. Along the coasts sea level fluctuations reflected local steric processes taking place in their vicinity. This effect was stronger on the western basin, whereas the coasts of the Eastern Mediterranean arise as the most suitable proxies for basin wide long term (> 60days) mean sea level (or ocean bottom pressure) changes at non-seasonal periods.

Keywords: Mediterranean Sea; sea level; ocean bottom pressure

Highlights:

- Rapid (<2 months) ocean bottom pressure oscillations in the Mediterranean Sea are coherent with sea level and decoupled between western an eastern subbasins.

- Low frequency steric sea level variability is larger in the western than in the eastern subbasin.

- Coastal sea level changes in the Eastern Mediterranean are representative of basin wide ocean mass changes for non-seasonal periods longer than 60 days.

1 Introduction

Knowledge of ocean bottom pressure (P_b) variability in combination with sea level changes provides information on the vertical structure of the ocean and on the water mass distribution. Not surprisingly, the number of studies on the relationship between P_b (or ocean mass) and sea level has grown in the last decade thanks to the confluence of various factors: on the one hand, the increasing availability of long term three-dimensional numerical simulations that provide joint P_b and sea level fields; on the other, an increasing number of P_b observations, including point-wise open ocean sensors but also the valuable and fruitful space gravimetry observations from the Gravity Recovery and Climate Experiment (GRACE) mission (Tapley et al, 2004); and in addition to that, the maturity reached by the processing and analysis of nearly global sea level altimetric measurements, starting in 1992. The relationship between P_b and sea level depends on the oceanic response to a given forcing; in a homogeneous ocean (no density changes in the water column) such response is depth-independent (Gill and Niiler, 1973). The relative weight of this barotropic response with respect to the depth-dependent (steric) processes changes with latitude and time scales. Earlier model based studies have established that at short time scales (<~100 days) sea level and P_b are very much related everywhere in the global ocean, with some exceptions as in the Tropics and in strongly eddying regions (Vinogradova et al., 2007; Bingham and Hughes, 2008; Quinn and Ponte, 2012). Conversely, at longer (intra- to interannual) time scales sea level variance is not generally explained by P_b variance as ocean variability is mostly related to steric processes over most parts of the ocean (Köhl and Stammer, 2008; Vinogradova et al., 2007; Bingham and Hughes, 2012). This was also confirmed by the combination of monthly altimetric and space gravimetry observations at inter-annual time scales (Piecuch et al, 2013). It must be mentioned here that, at certain spatial and temporal scales, steric processes can also impact P_b (e.g. Song and Zlotnicki, 2004). Some regions have, however, been identified where P_b and sea level changes show a correspondence even at long time scales, namely shallow and shelf areas and semi-enclosed basins (Piecuch and Ponte, 2011). This is the case of the Mediterranean Sea, which has been identified as one of the few regions worldwide where basin average water mass (P_b) changes explain to large extent sea level variability (Bingham and Hughes, 2008; Piecuch et al, 2013).

The Mediterranean Sea is a semi-enclosed basin located at mid-latitudes and connected to the Atlantic Ocean through the narrow Strait of Gibraltar. Given its relatively well monitored coastal sea level, it has been an important region for assessment of global sea level trends, glacio-isostatic adjustment and tectonic processes, among other issues. Mean sea level variability in this region has been extensively investigated based on in-situ and remote observations (Tsimplis and Baker, 2000; Tsimplis and Rixen, 2002; Fenoglio-Marc, 2002; Criado-Aldeanueva et al, 2008; Marcos and Tsimplis, 2008; Calafat and Gomis, 2009; Marcos and Tsimplis, 2009; Tsimplis et al, 2013) as well as using numerical models (Somot and Colin, 2008; Gomis et al, 2008; Sannino et al 2009; Calafat et al, 2012). Consequently, it has been well documented that basin wide inter-annual and longer term mean sea level oscillations are mostly driven by mass variations (Fukumori et al 2007; Calafat et al, 2010; Landerer and Volkov, 2013) attributed to exchanges through the Strait of Gibraltar. These are forced either by local processes such as winds at Gibraltar or steric changes in the nearby Atlantic, or by a remote forcing, like changes in the atmospheric pressure over the North Atlantic Ocean or mass addition from land-based ice melting (Fukumori et al, 2007; Calafat et al, 2012; Tsimplis et al 2013; Pinardi et al, 2014). Indeed, earlier works addressing mass variability, or alternatively P_b changes, in the Mediterranean Sea have mostly addressed basin average changes, despite the Mediterranean Sea being a deep basin with its own ocean circulation and dynamics (see e.g. Schroeder et al, 2013). Fukumori et al (2007) is one of the exceptions, since their study made use of an ocean circulation model covering the Mediterranean Sea and a sector of the Northeast Atlantic. However, the coarse model resolution (1ºx1º) impeded accounting for the steric processes dominated by mesoscale signals. Other works with a global focus have also provided insight into the relationship between P_b and sea level in the Mediterranean (Vinogradova et al, 2007; Bingham and Hughes, 2008).

The aim of the present work is to explore and quantify P_b variability in the Mediterranean Sea at different time scales and to clarify its relationship with sea level at the regional and local scales. The presence of steric processes, especially in some parts of the basin where active mesoscale variability with presence of eddies takes place, is expected to break the coherence observed between spatially averaged P_b and sea level, at least at the inter-annual and longer time scales. To achieve this goal an eddy-permitting numerical ocean model has been used. The high spatial resolution in the model is required to resolve the small scale structures in the Mediterranean Sea, where the baroclinic Rossby radius is only a few tens of kilometres, and to explore the relationship between sea level and P_b at different spatial and temporal scales. In this sense, the present work represents a step further with respect to the aforementioned studies by Fukumori et al (2007), Vinogradova et al (2007) and Bingham and Hughes (2008), in which the horizontal resolution was between 0.25º and 1º and did not allow for a proper representation of the topography of the Mediterranean Sea.

This paper is organized as follows: in Section 2 the numerical model is presented together with the methodology used throughout the paper. Section 3 is devoted to the results, which include the characterization of the P_b variability in the Mediterranean Sea, the rapid P_b fluctuations, the seasonal cycle of P_b and the low frequency behaviour. The last section summarizes the major findings and discusses its implications as well as the limitations of the present work.

2 Numerical model and methods

Daily outputs of temperature (T), salinity (S) and sea surface height (ssh) fields were obtained from an ocean reanalysis for the period 1999-2011 carried out by the Mediterranean Forecasting System at INGV and freely available at MyOcean web site (http://www.myocean.eu/, product ID MEDSEA_REANALYSIS_PHYS_006_004). In this particular simulation the ocean model NEMO was implemented in the Mediterranean Sea and a nearby sector of the Atlantic Ocean with a spatial resolution of 1/16º x 1/16º in latitude and longitude and 72 unevenly spaced vertical levels (Oddo et al., 2009). The regional model was nested to a global model (Drevillon et al., 2008) in the Atlantic box using the Flather boundary conditions (Flather, 1976) for vertically integrated velocities. This implies that the regional model is not conserving its volume and mass. In order to ensure global mass conservation the global spatial mean steric anomalies should be added to ssh at each time step (Greatbach, 1994; Ponte, 1999; Griffies and Greatbach, 2012). Unfortunately this correction for the global model was not available and therefore was not applied. Nevertheless, it is expected to be small in comparison with regional changes and minimized by the fact that the analyses have been performed on detrended time series. This numerical setup has been evaluated in earlier works. Oddo et al. (2009) compared modelled T with Argo data and modelled ssh with tide gauge and satellite altimetry and demonstrated the improvement in the nesting with respect to a closed model in terms of the characteristics of the outflow waters and the seasonal sea level variability. Adani et al (2011) assessed the quality of an 18-years simulation in terms of hydrographic properties and sea level anomalies with the aim of exploring two different data assimilation schemes. Their analyses resulted in a preferred scheme that was then used in this product.

Daily fields of ocean bottom pressure P_b were computed at each grid point as:

$$P_b = \int_{-H}^{0} \rho g dz + \int_{0}^{\eta} \rho_0 g dz = \int_{-H}^{0} \rho g dz + \rho_0 g \eta \quad (1)$$

Where ρ is the ocean density, computed using T and S, ρ_0 is the density at the sea surface, H is the water depth, η is the sea surface elevation and g is the gravity acceleration. Neither the regional model nor the global model to which it is nested at the boundaries are forced by atmospheric pressure and, therefore, the term is not accounted for in this equation. The first term in the right hand side of equation (1) corresponds to the steric contribution. Likewise, the thermosteric (halosteric) term is defined using the same expression but with ρ determined only by T (S) changes and S (T) being kept constant at its initial value. P_b anomalies are computed by removing its time-mean field and are then normalized into water height equivalent as:

$$\frac{P_b - \overline{P_b}}{\rho_0 g}$$

The percentage of variance of sea level explained by P_b was computed as:

$$\frac{1 - var(ssh - P_b)}{var(ssh)} \times 100$$

When stated in the text, as part of the analysis daily values of ssh and P_b fields were high-passed filtered using a Butterworth filter of order 2. The low-passed component of each variable was then estimated by subtracting the high-passed filtered series to the total signal. The mean seasonal cycle was obtained by fitting an annual and a semi-annual signal to the low-passed component using harmonic analysis.

Additionally, daily 10-m wind fields were obtained from ERA-Interim (European Centre for Medium-Range Weather Forecasts – ECMWF - Re-Analysis), available at the ECWMF web site (http://data-portal.ecmwf.int/data/d/interim_daily/). The wind fields are the same that were used to force the model.

3 Results

3.1 Scales of variability of P_b in the Mediterranean Sea

Standard deviations of detrended daily P_b and sea level anomalies are mapped in Figure 1. P_b variability ranges between 4 and 8 cm, whereas sea level presents higher values up to 12 cm. These results are qualitatively in agreement with those inferred for the Mediterranean Sea in the global analyses of Vinogradova et al (2007) and Bingham and Hughes (2008). Spatially averaged sea level variability is higher (7.9 cm) than P_b variability (6.2 cm). According to numerical results, the Mediterranean Sea is a region with large P_b variance in comparison with the global ocean, where the range of P_b anomalies is around 1 cm or less at these time scales (Bingham and Hughes, 2008). Larger variability in sea level is found at regions of intense mesoscale activity (i.e. strong presence of eddies), such as along the African coast in Western Mediterranean following the Algerian Current, and south of Crete in Eastern Mediterranean. It is thus concluded that the spatial distribution of sea level variability is primarily due to the regional distribution of steric processes. In the case of P_b, larger variability is confined to coastal and shallow areas. Part of these coastal P_b signal is originated by the water redistribution over the topography towards shallow areas induced by open ocean steric changes (Landerer et al., 2007; Bingham and Hughes, 2012). It is noticeable that P_b variability in the western basin (5.3 cm) is smaller than in the eastern basin (6.7 cm), whereas this difference is not apparent in sea level.

When basin averages were computed, local steric processes were filtered out and the basin wide mean sea level signal showed high correspondence with its barotropic component (Figure 2). This is an expected result, since for increasing spatial scales at a fixed frequency the oceanic response becomes increasingly depth- independent (Gill and Niiler, 1973; Frankignoul et al., 1997). The correlation between the two curves was 0.75. A spectral analysis was performed on both curves using a Hamming window with length 2^{11} days (Figure 2b). Results revealed that the energy content of sea level and P_b was almost the same for the high frequencies and differed at the lower frequencies (at the 95% confidence level). A cut-off period of 60 days was defined in order to examine separately the high and the low frequency components. Overall, the contribution of the high frequency fluctuations to P_b variability is smaller (standard deviation of 1.7 cm) than that of the low frequency (5.4 cm); however, the latter is largely contributed by the seasonal cycle (3.2 cm when deseasoned), as expected from the prominent seasonal oscillations observed in Figure 2a.

It must be recalled that P_b accounts for changes in total ocean mass, that is, fresh water and salt content. The contribution of the salt content (halosteric term) to P_b was computed and it was found that its standard deviation was only 0.3 cm, that is, much smaller than the standard deviation of the basin average P_b (6.2 cm). Thus, the contribution of changes in the salt content to P_b variability is negligible in comparison with the contribution of water mass changes. Interestingly though, basin average P_b displays a linear trend during the modelled period of 6.7±0.3 mm/yr, that is entirely accounted for by the halosteric term, indicative of a gradual increase of salt content. Whether this trend in the model is realistic or not does not affect the calculations presented in this work and the determination of its origin is certainly beyond the scope of the present study.

3.2 Rapid P_b fluctuations

Rapid P_b and sea level variations were correlated using high-passed filtered time series with a cut-off period of 60 days (Figure 3). There is a clear evidence that high frequency sea level oscillations are mostly barotropic in the Mediterranean Sea, in line with results for most of the global ocean (Vinogradova et al, 2007; Bingham and Hughes, 2008). The basin average standard deviations of P_b and sea level are 2.2 and 2.5 cm, respectively, thus nearly the same. At these time scales the sea level variance explained by P_b was larger than 85% over half of the basin. The explained percentage would be even higher if the atmospheric pressure forcing was included in the modeled sea level variability. The southern sector of the western basin, where high energy mesoscale eddies activity has been reported (Millot et al, 1997), displayed correlations below 0.8. In spite of this, the values were still relatively high and the sea level variance explained by its barotropic component was more than 50%, except along the African coast in the path of the Algerian Current. Particularly low correlations were found along the Southern coast of the Iberian Peninsula, an area under the direct influence of the

Atlantic inflow (see e.g. Viúdez et al, 1998). Such distinct behaviour of coastal sea level at this site corroborates that it is not representative of any regional sea level, as previously pointed out by Marcos and Tsimplis (2008).

Correlations between sea level at two coastal sites, one on each subbasin, and P_b over the domain were computed (Figure 4). According to Figure 3, high-passed filtered coastal sea level and P_b at the two selected points are equivalent and sea level was preferred because it is the variable usually measured at the coast. The results, mapped in Figure 4, revealed an interesting feature: rapid P_b oscillations are uncorrelated between the eastern and the western subbasins, separated by the natural boundary at the Strait of Sicily. Within each subbasin, high frequency P_b changes are highly coherent and can be represented by any local point-wise measurement. These subbasin modes are stationary, as the maxima correlations among grid points were found at zero lag. The same picture was found when deep ocean points were used instead of coastal locations, thus reaffirming that rapid P_b oscillations are coherent within each subbasin. This result contrasts with the single basin wide oscillation reported by Fukumori et al (2007); the discrepancy is explained by the coarser spatial resolution of their model (1º) which does not represent the detailed topography at subbasin scale and by the fact that they did not high-passed filter the data and, thus, the longer term P_b oscillations could mask the higher frequency changes.

The decoupling between subbasins is suggestive of a topographic effect. In order to identify the signals, spatial averages over the western and eastern subbasins of high-passed filtered P_b were computed and analysed separately using spectral and wavelet analyses. Power spectra were computed using a Hamming window with length 2^{10} (Figure 5a). Only the frequency band between 2 and 125 days has been plotted in order to focus on the rapid oscillations. Results show that the two subbasins present different energy distribution, with the eastern basin peaking at 41 days and the western basin at 48 and 31 days with lower energy content. A wavelet analysis was also carried out. The mother function used was Morlet and the energy contents between 5 and 200 days were represented (Figure 6). The results revealed that oscillations occur simultaneously in the two subbasins, which is indicative of a common forcing. Despite the resemblance of the temporal variability of the signals, they differed in intensity and, more remarkably, in their frequency, in agreement with spectral analyses. The origin of these rapid P_b fluctuations was explored using zonal wind stress from a grid point at the Atlantic side of the Strait of Gibraltar. A wavelet analysis was performed onto the time series in the same way as for subbasin averaged P_b (Figure 6, top).. The resulting distribution of energy resembled that of the P_b at the frequency bands where fluctuations were observed. Indeed, when the coherence between subbasin averaged P_b time series and zonal wind stress was computed (Figure 5b), it was found to be maximum at the frequency band between 35 and 55 days. These results demonstrate that energy pulses in local zonal wind stress had a response in terms of rapid barotropic oscillations in the entire basin. The wind stress at Gibraltar transmits energy to the basin in the form of P_b oscillations, which in turn excite the natural modes of the two subbasins. This mechanism is thus similar to the generation of seiche oscillations, typically observed at small coastal inlets. In the case of the Mediterranean Sea, the two subbasins act as a system of coupled oscillators, separated by the Strait of Sicily. This implies that the natural modes of each subbasin, defined by the topographic features, are affected by the presence of the other subbasin, as demonstrated by Marcos et al (2005) for a system of small inlets.

3.3 Seasonal cycle of P_b

The mean seasonal cycle was computed at each grid point using P_b and sea level time series low-passed filtered with a cut-off period of 60 days. Amplitudes and phases of the annual cycle are mapped in Figure 7. It is remarkable that the mean annual signal in P_b was significantly smaller in the western basin (2.3 cm on average) than in the eastern basin (4.2 cm on average), with nearly constant values within each subbasin. The smaller annual cycle in the western basin is partly responsible of the lower values of standard deviation of non-filtered P_b shown in Figure 1. Conversely, annual amplitudes of sea level displayed a high spatial variability, but without significant differences between subbasins. Annual phases were fairly constant over the entire domain for both P_b and sea level. While P_b mean annual cycle peaked by the end of November, the annual cycle of sea level reached its maximum at beginning of October. These results are consistent with the annual sea level cycle being predominantly of steric origin and resulting from the combination of two sinusoidal-like signals, one peaking in September associated with thermal expansion/contraction due to heat fluxes at the sea surface and another peaking in December and representing the water mass variations within the basin (Marcos and Tsimplis, 2007; Fenoglio-Marc et al, 2012). The differences in the mean annual cycle of sea level and P_b are in agreement with the lack of coherency between the two signals reported by Bingham and Hughes (2008). In contrast, Vinogradova et al (2007) found coherency at the annual period over most of the Mediterranean basin, probably due to a bad representation of the topography of the basin in their coarse resolution global model.

The average amplitude of P_b annual cycle is 3.6 cm, in the upper range of the values derived from GRACE observations over the Mediterranean Sea with different corrections for the continental hydrology contribution (Calafat et al, 2010; García et al, 2010; Fenoglio-Marc et al, 2012). In comparison with global values, the Mediterranean Sea exhibits larger annual P_b changes (Johnson and Chambers, 2013). On top of that, Johnson and Chambers (2013), using the last generation of GRACE data, quantified the annual amplitude of P_b in the Northeast Atlantic as low as 0.5-1 cm. This discrepancy between the annual amplitudes in the Mediterranean and those measured in the nearby Atlantic points towards a different origin of the seasonality in the basin. Indeed, according to Soto-Navarro et al (2010), the mass-induced annual signal in the Mediterranean Sea is driven by changes in evaporation, precipitation and river run-off, among which the former is the dominant (Mariotti, 2009).

In contrast with the annual signal, the semi-annual cycle in sea level and P_b were essentially identical (not shown). In other words, semi-annual sea level variations in the Mediterranean Sea are barotropic.

3.4 Low frequency variability of P_b

Low frequency variability was examined using low-passed filtered with a cut-off period of 60 days and deseasoned sea level and P_b fields. Point-by-point correlations are mapped in Figure 8a. Overall, correlations are much lower than for high frequencies (Figure 3), as expected since the oceanic response becomes increasingly depth-dependent for increasing periods at a given spatial scale (Gill and Niiler, 1973; Frankignoul et al, 1997). Over shallow areas and along most of the coasts, P_b explains more than 90% of the local variance of sea level, indicative of the barotropic nature of sea level oscillations in shallow waters (Bingham and Hughes, 2012). Once again, as in the high frequency, this was not the case along the southern Iberian coast, where even coastal sea level was found to respond to the strong steric changes in the area associated with inflow of Atlantic surface waters. Also, poor correspondence was found in the southern Ionian and Levantine basins and over most of the deep part of the western basin. In Central Mediterranean P_b explains more than 50% of the low frequency sea level variance. The lower correspondence between sea level and P_b in the western basin is indicative of the presence of larger steric changes than in the eastern basin. Overall, the correlations found are large in comparison with other regions in the world ocean of similar depths (Bingham and Hughes, 2008; Piecuch et al, 2013).

The non-seasonal low frequency variability was also explored (Figure 8b-c). Standard deviations ranged between 2 and 7 cm for sea level and less than 4 cm for P_b. It is worth noting that P_b values in the western basin were still smaller (2.9 cm) than in the eastern basin (3.6 cm). The averaged difference has therefore reduced from 1.5 cm to 0.7 cm. This may respond to the fact that only the mean seasonal cycle was removed, despite significant inter-annual changes in the annual and semi-annual sea level signals have been previously reported in the Mediterranean Sea (Marcos and Tsimplis, 2007).

In order to address the question of to which extent low frequency P_b variations are coherent within the basin, the correlations between sea level at two single deep ocean grid points and P_b over the rest of the domain were evaluated (Figure 9). Correlations higher than 0.7 were found almost everywhere, which demonstrated that the P_b signal appears coherent within the domain. Lower correlations (although still significant at the 95% confidence level) were found along coastal locations. The reason is that coastal P_b variability is influenced by steric changes in the deep ocean that induced bottom pressure changes (i.e. water mass redistribution) in shallow waters (Landerer et al, 2007; Bingham and Hughes, 2012). As observations are by far more frequent along the coast, the extent to which this P_b signal can be captured by coastal sea level records was also investigated. The same two locations as in Section 3.2 were chosen; as for the high frequency, low-pass filtered sea level and P_b were essentially the same at these two coastal sites (correlation of 0.97). The resulting correlations between coastal and open ocean P_b, mapped in Figure 10, revealed a surprising feature: coastal sea level (or P_b) in the Levantine basin showed high (>0.8) correlations with P_b changes over the eastern basin and also over the western basin (>0.7, except in central western basin); on the contrary, coastal sea level in the western basin displayed lower correlations with local P_b changes, even in its surroundings. This behaviour was not limited to the particular locations chosen in Figure 10, but could be extrapolated to the rest of the coasts in each subbasin as will be shown later in the discussion section. When instead of P_b, sea level was correlated, the area coherent with coastal sea level was larger (not shown). The interpretation of these results suggested that sea level changes along the coasts of the Western Mediterranean Sea were dominated by water redistribution induced by local steric processes. This finding is in line with results shown in Figure 8, which indicate that steric processes are more relevant in the western than in the eastern basin.

In spite of the low correlations between sea level and P_b at the local scales found over many parts of the Mediterranean (Figure 8a), when the basin averages were calculated they displayed an excellent correspondence. The correlation between low-passed filtered and deseasoned basin average sea level and P_b was 0.95. Likewise, subbasin P_b averages were also consistent to each other, with correlation 0.87; a similar correspondence was found for subbasin average sea level, with a correlation of 0.83.

4 Discussion and Conclusions

The spatial and temporal distribution of ocean bottom pressure (P_b) variability in the Mediterranean Sea has been characterized and its relationship with sea level changes assessed. The use of a high resolution (1/16ºx1/16º in latitude and longitude) numerical ocean model has allowed accounting for mesoscale processes within the basin that dominate the spatial distribution of sea level variability away from the coast. In line with earlier investigations (Calafat et al, 2010; Tsimplis et al, 2013; Landerer and Volkov, 2013; Piecuch et al, 2013), it has been confirmed that basin average sea level changes in the Mediterranean Sea are predominantly barotropic at all time scales, a characteristic usually reserved to shallow environments. The only exception that should be recalled is the sea level annual cycle, which is dominated by the steric signal and whose barotropic contribution is clearly different in amplitude and phase. Basin wide P_b changes in the Mediterranean Sea essentially reflect water mass variations. Although changes in salt content must also be accounted for (Jordà and Gomis, 2013), these were only relevant for the long term trends and negligible on the daily to inter-annual time scales explored in the present study.

Rapid sea level fluctuations (with periods less than two months) are mostly barotropic, not only on average, but also locally. Such sea level oscillations occur simultaneously everywhere in the basin, thus indicating a common forcing mechanism. A good correspondence was found with zonal wind forcing in the Strait of Gibraltar, in agreement with Fukumori et al (2007). However, the western and eastern subbasins are decoupled, as sea level and P_b variations with periods of the order of a few days are constrained by the topographic characteristics of both basins. It is worth recalling that atmospheric pressure changes, which may be responsible for a large fraction of the high frequency sea level and P_b variability, are not included in the model forcing.

At monthly and longer time scales steric changes can be an important contributor to sea level variability locally, especially over the western basin. Away from the coast, steric changes break the coherency between sea level and P_b, and high correlations were confined over shallow areas and at coastal locations. Hence, sea level at any location in the deep part of the basin results from the addition of a spatially coherent mass-induced component and the local steric variability. The latter was filtered out when the basin average was computed, in agreement with the linear theory of the large-scale oceanic adjustment (Gill and Niiler, 1973; Frankignoul et al, 1997).

Along the coasts the picture is more complex, as hinted from Figure 10. An evaluation of the ability of coastal sea level to account for basin average P_b changes was extended to all coastal sites. The correlations between low frequency coastal sea level and basin average P_b (Figure 11a) define a clear geographical pattern. The lack of correlation could be anticipated at the few sites where coastal sea level changes were not barotropic (northern Alboran Sea, as evidenced in Figure 8a). For the rest of the coastal domain, despite coastal sea level changes were entirely barotropic, they are not everywhere dominated by basin wide P_b variability. This is the case of most of the Western Mediterranean coasts (Spanish coast, Gulf of Lions, Balearic Islands, Corsica and Sardinia) and the Gulf of Gabes. By contrast, correlations as high as 0.9 were found along the coasts of the Eastern Mediterranean, the Aegean and the Adriatic Seas. In the former case, coastal sea level fluctuations reflected P_b signals induced by small scale steric processes; in the latter, coastal sea level was a good indicator of the long term basin wide P_b (or sea level) changes. A coherence analysis between coastal sea level and basin averaged P_b was carried out for selected points (black dots in Figure 11a) in order to check whether this behaviour also holds at the lowest frequencies resolvable by the model (Figure 11b). The results evidenced that in the areas of higher correlation (longitudes > 15ºE) the coherence was maximum for the entire range of frequencies; conversely, in the westernmost areas the coherence was lower and maximum around the annual cycle. Note that although the series are deseasoned, only the mean seasonal cycle was removed, as pointed out above. The reason for the difference between areas of high and low correlations is that steric changes represent a larger part of sea level variability in the western than in the eastern basin (Figure 8a). At the coast the sea level signal is almost entirely barotropic and reflects both P_b and steric changes in the nearby deep locations. Thus, the smaller the steric changes the higher the coherence between coastal and open ocean P_b.

The Mediterranean Sea is one of the few regions worldwide where mass-induced sea level changes appear coherent over a deep and relatively large area and match averaged sea level variations at inter-annual time scales. The variability of the mass-induced sea level component is large in comparison with other deep regions in the global ocean, as it is mainly related to exchanges through the Strait of Gibraltar driven by local sea level changes in the nearby Atlantic. Such coherent mode of P_b variability can be easily monitored at selected coastal sites, which have arisen as suitable proxies for basin wide sea level changes. This is an important issue to consider when Mediterranean tide gauge observations are used in a global context. The feasibility of accurate P_b and sea level observations suggests that the Mediterranean Sea is a particularly convenient place for comparison of multiple platform sea level observations and its components. Sea level in the Mediterranean is monitored by a dense network of coastal tide gauges as well as by satellite altimetry, which is currently fully developed and provides accurate sea level measurements at the regional scale. The strong link between sea level and basin wide P_b is a useful constraint to improve the still limited space gravimetry observations at the regional scale. For example, the required corrections of hydrological variations leaking into the ocean could benefit from this fact.

Finally, the limitations of the present study must be emphasized. The close relationship between Mediterranean sea level and P_b found at daily to inter-annual temporal scales does not necessarily hold for the long term (decadal and longer time scales). Gradual changes in the salt content of the basin would induce an increase of P_b without a sea level counterpart. This circumstance is, according to modelling studies, a plausible situation in the future evolution of the Mediterranean Sea under climate change scenarios (Somot et al, 2008). In consequence, sea level and P_b act as two fundamental and complementary environmental variables at these time scales.

Acknowledgements: The data used in this study were generated using MyOcean products. M. Marcos acknowledges a ‘‘Ramon y Cajal’’ contract funded by the Spanish

Ministry of Economy. The author is also grateful to P. Oddo for his help with modelling questions, to A. Amores for computing assistance and to F.M. Calafat, D. Gomis, S. Monserrat and J. Williams for comments on the manuscript.

References

Adani, M., S. Dobricic, N. Pinardi (2011), Quality Assessment of a 1985–2007 Mediterranean Sea Reanalysis. J. Atm. Oc. Tech., 28, 569-589, doi: 10.1175/2010JTECHO798.1

Bingham, R. J., and C. W. Hughes (2008), The relationship between sea-level and bottom pressure variability in an eddy permitting ocean model, Geophys. Res. Lett., 35, L03602, doi:10.1029/2007GL032662

Bingham, R. J., and C. W. Hughes (2012), Local diagnostics to estimate density-induced sea level variations over topography and along coastlines, J. Geophys. Res., 117, C01013, doi:10.1029/2011JC007276

Calafat, F.M., Gomis, D. (2009), Reconstruction of Mediterranean Sea level fields for the period 1945–2000. Global Planet. Change 66 (3–4), 225–234. doi:10.1016/j. gloplacha.2008.12.015

Calafat, F. M., M. Marcos, and D. Gomis (2010), Mass contribution to the Mediterranean Sea level variability for the period 1948–2000, Global Planet. Change, 73, 193–201, doi:10.1016/j.gloplacha.2010.06.002

Calafat, F. M., G. Jordà, M. Marcos, and D. Gomis (2012), Comparison of Mediterranean sea level variability as given by three baroclinic models, J. Geophys. Res., 117, C02009, doi:10.1029/2011JC007277

Criado-Aldeanueva, F., J. Del Río Vera, and J. García-Lafuente (2008), Steric and mass-induced Mediterranean sea level trends from 14 years of altimetry data, Global Planet. Change, 60, 563 – 575, doi:10.1016/j.gloplacha.2007.07.003

Drevillon, M., Bourdallé-Badie, R., Derval, C., Drillet, Y., Lellouche, J. M., Rémy, E., Tranchant, B., Benkiran, M., Greiner, E., Guinehut, S., Verbrugge, N., Garric, G., Testut, C. E., Laborie, M., Nouel, L., Bahurel, P., Bricaud, C., Crosnier, L., Dombrosky, E., Durand, E., Ferry, N., Hernandez, F., Le Galloudec, O., Messal, F., and Parent, L. (2008), The GODAE/MercatorOcean global ocean forecasting system: results, applications and prospects, J. Operational Oceanogr., 1(1), 51–57.

Fenoglio-Marc, L. (2002), Long-term sea level change in the Mediterranean Sea from multi-satellite altimetry and tide gauges, Phys. Chem. Earth, 27, 1419 – 1431.

Fenoglio-Marc, L., R. Rietbroek, S. Grayek, M. Becker, J. Kusche, E. Stanev, (2012), Water mass variation in the Mediterranean and Black Seas. J. Geodyn., 59-60, 168-182, 10.1016/j.jog.2012.04.001

Flather, R. A. (1976), A tidal model of the northwest European continental shelf, Memories de la Societe Royale des Sciences de Liege, 6(10), 141–164.

Frankignoul, C., et al., (1997), A Simple Model of the Decadal Response of the Ocean to Stochastic Wind Forcing. Journal of Physical Oceanography, 27, 1533-1546.

Fukumori, Ichiro, Dimitris Menemenlis, Tong Lee, (2007), A Near-Uniform Basin-Wide Sea Level Fluctuation of the Mediterranean Sea. J. Phys. Oceanogr., 37, 338–358. doi: http://dx.doi.org/10.1175/JPO3016.1

García-García, D., B.F. Chao, and J.-P. Boy (2010), Steric and mass-induced sea level variations in the Mediterranean Sea revisited, J. Geophys. Res., 115, C12016, doi:10.1029/2009JC005928

Gill, A. E., and P. P. Niiler, (1973), The theory of the seasonal variability in the ocean. Deep-Sea Research, 20, 141-177.

Gomis, D., Ruiz, S., Sotillo, M.G., Álvarez-Fanjul, E., Terradas, J., (2008), Low frequency Mediterranean Sea level variability: the contribution of atmospheric pressure and wind. Global Planet. Change 63, 215–229. doi:10.1016/j.gloplacha.2008.06.005

Greatbatch, R. J., (1994), A note on the representation of steric sea level in models that conserve volume rather than mass. Journal of Geophysical Research, 99, C6.

Griffies, SM., R.J. Greatbatch, (2012), Physical processes that impact the evolution of global mean sea level in ocean climate models Ocean Modelling 51, 37–72

Johnson, G. C., and D. P. Chambers (2013), Ocean bottom pressure seasonal cycles and decadal trends from GRACE Release-05: Ocean circulation implications, J. Geophys. Res., 118, 4228–4240, doi:10.1002/jgrc.20307

Jordà, G., and D. Gomis (2013), On the interpretation of the steric and mass components of sea level variability: The case of the Mediterranean basin,J. Geophys. Res., 118, 953–963, doi:10.1002/jgrc.20060

Köhl, Armin, Detlef Stammer, (2008), Decadal Sea Level Changes in the 50-Year GECCO Ocean Synthesis. J. Climate, 21, 1876–1890. doi: http://dx.doi.org/10.1175/2007JCLI2081.1

Landerer, F. W., J. H. Jungclaus, and J. Marotzke (2007), Ocean bottom pressure changes lead to a decreasing length-of-day in a warming climate, Geophys. Res. Lett., 34, L06307, doi:10.1029/2006GL029106

Landerer, F. W., and D. L. Volkov (2013), The anatomy of recent large sea level fluctuations in the Mediterranean Sea, Geophys. Res. Lett., 40, 553–557, doi:10.1002/grl.50140.

Marcos, M., S. Monserrat, R. Medina, P. Lomónaco (2005), Response of a harbor with two connected basins to incoming long waves. App. Oc. Res., 27, 209-215, doi:10.1016/j.apor.2005.11.010

Marcos, M., and M. N. Tsimplis (2007), Variations of the seasonal sea level cycle in southern Europe, J. Geophys. Res., 112, C12011, doi:10.1029/2006JC004049

Marcos, M., and M. Tsimplis (2008), Coastal sea level trends in southern Europe, Geophys. J. Int., 175,70–82, doi:10.1111/j.1365-246X.2008.03892.x

Mariotti, A. (2009), Recent changes in the Mediterranean water cycle: A pathway towards toward long ‑ term regional hydroclimatic change?. J. Clim., 23, 1513–1525

Millot, C., Taupier-Letage, I., Benzohra, M., (1997), Circulation off Algeria inferred from the Médiprod-5 current meters, Deep-Sea Res. 44 (9-10), 1467-1495.

Oddo, P., Adani, M., Pinardi, N., Fratianni, C., Tonani, M., Pettenuzzo, D. (2009), A nested Atlantic-Mediterranean Sea general circulation model for operational forecasting, Ocean Sci., 5, 461–473.

Piecuch, C. G., and R. M. Ponte (2011), Mechanisms of interannual steric sea level variability, Geophys. Res. Lett., 38, L15605, doi:10.1029/2011GL048440

Piecuch, C. G., K. J. Quinn, and R. M. Ponte (2013), Satellite-derived interannual ocean bottom pressure variability and its relation to sea level, Geophys. Res. Lett., 40, 3106–3110, doi:10.1002/grl.50549

Pinardi, N., A. Bonaduce, A. Navarra, S. Dobricic, P. Oddo, (2014), The mean sea level equation and its application to the Mediterranean Sea. J. Clim., 27, 442-447, 10.1175/JCLI-D-13-00139.1

Ponte, R. M., (1999), A preliminary model study of the large-scale seasonal cycle in bottom pressure over the global ocean. Journal of Geophysical Research, 104, C1.

Quinn, K, J., and R. M. Ponte, (2012), High frequency barotropic ocean variability observed by GRACE and satellite altimetry. Geophysical Research Letters, 39, L07603.

Sannino, G., M. Herrmann, A. Carrillo, V. Rupolo, V. Ruggiero, V. Artale, and P. Heimbach (2009), An eddy-permitting model of the Mediterranean Sea with a two-way grid refinement at the Strait of Gibraltar, Ocean Modell., 30,56–72, doi:10.1016/ j.ocemod.2009.06.00

Schroeder, K., García-Lafuente, J., Josey, S.A., Artale, V., Buongiorno Nardelli, B., Carrillo, A., Gacic, M., Gasparini, G.P., Herrmann, M., Lionello, P., Ludwig, W., Millot, C., Özsoy, E., Pisacane, G., Sánchez-Garrido, J.C., Sannino, G., Santoleri, R., Somot, S., Struglia, M., Stanev, E., Taupier-Letage, I., Tsimplis, M.N., Vargas-Yáñez, M., Zervakis, V., Zodiatis, G., 2013. Circulation of the Mediterranean Sea and its variability. In The Climate of the Mediterranean Region: From the Past to the Future, pp 187-238 Ed. Piero Lionello, Elsevier, ISBN 978-0-12-398466-1

Somot, S., and J. Colin (2008), First step towards a multi-decadal high resolution Mediterranean Sea reanalysis using dynamical downscaling of ERA40. Research activities in atmospheric and oceanic modeling, Rep. 38, Working Group on Numer. Exper., Geneva, Switzerland.

Somot, S., F. Sevault, M. Déqué, and M. Crépon (2008), 21st century climate change scenario for the Mediterranean using a coupled atmosphere–ocean regional climate model, Global Planet. Change, 63,112–126, doi:10.1016/j.gloplacha.2007.10.003.

Song, Y. T., and V. Zlotnicki (2004), Ocean bottom pressure waves predicted in the tropical Pacific, Geophys. Res. Lett., 31, L05306, doi:10.1029/2003GL018980.

Soto−Navarro, J., F. Criado−Aldeanueva, J. García-Lafuente, and A. Sánchez−Román (2010), Estimation of the Atlantic inflow through the Strait of Gibraltar from climatological and in situ data, J. Geophys. Res., 115, C10023, doi:10.1029/2010JC006302

Tapley, B. D., S. Bettadpur, M. Watkins, and C. Reigber (2004), The Gravity Recovery and Climate Experiment: Mission overview and early results, Geophys. Res. Lett., 31, L09607, doi:10.1029/2004GL019920.

Tsimplis, M. N., and T. F. Baker (2000), Sea level drop in the Mediterranean Sea: An indicator of deep water salinity and temperature changes?, Geophys. Res. Lett., 27(12), 1731 – 1734, doi:10.1029/1999GL007004

Tsimplis, M. N., and M. Rixen (2002), Sea level in the Mediterranean Sea: The contribution of temperature and salinity changes, Geophys. Res. Lett., 29(23), 2136, doi:10.1029/2002GL015870

Tsimplis, M., G. Spada, M. Marcos, and N. Flemming (2011), Multi-decadal sea level trends and land movements in the Mediterranean Sea with estimates of factors perturbing tide gauge data and cumulative uncertainties, Global Planet. Change, 76,63–76, doi:10.1016/j.gloplacha.2010.12.002

Tsimplis, M. N., F. M. Calafat, M. Marcos, G. Jordà, D. Gomis, L. Fenoglio-Marc, M. V. Struglia, S. A. Josey, and D. P. Chambers (2013), The effect of the NAO on sea level and on mass changes in the Mediterranean Sea, J. Geophys. Res., 118, doi:10.1002/jgrc.20078

Vinogradova, N. T., R. M. Ponte, and D. Stammer (2007), Relation between sea level and bottom pressure and the vertical dependence of oceanic variability, Geophys. Res. Lett., 34, L03608, doi:10.1029/2006GL028588

Viúdez, A., Pinot, J.M., Haney, R.L., (1998), On the upper layer circulation in the Alboran Sea. Journal of Geophysical Research 103 (C10), 21,653–21,666. http://dx.doi.org/10.1029/98JC01082

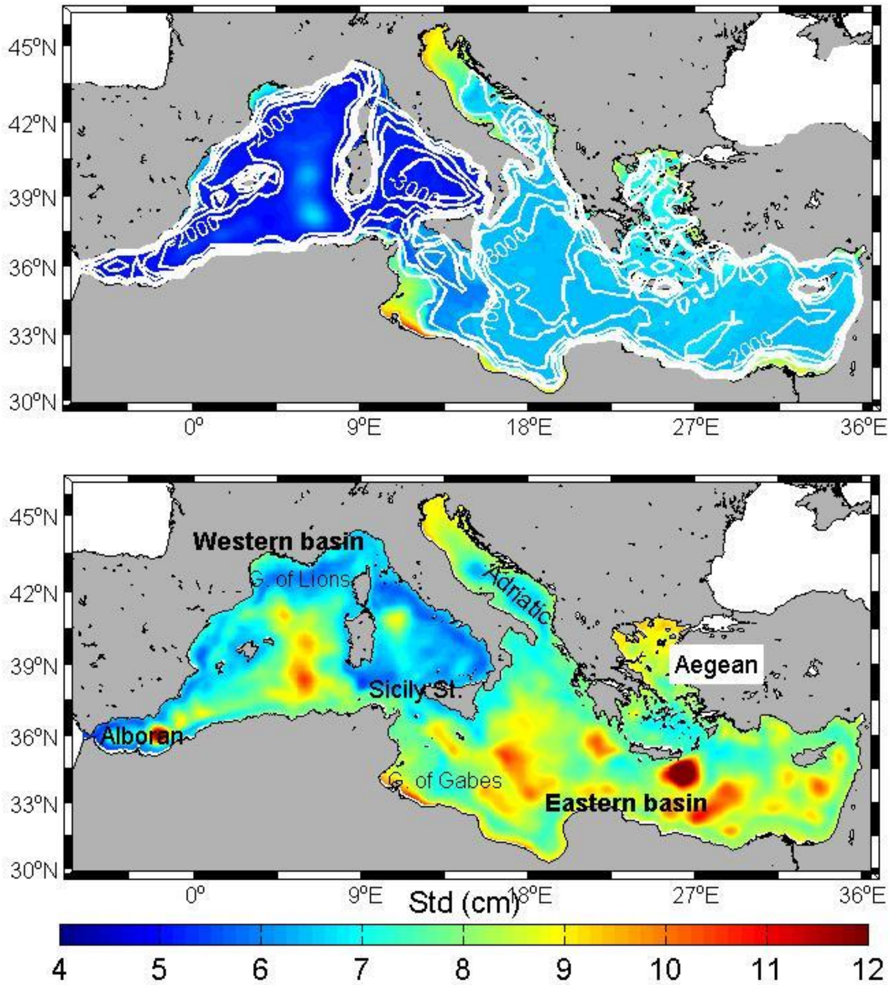

Figure 1. Standard deviations of daily detrended P_b (top) and sea level (bottom). The bathymetry is included in the top map.

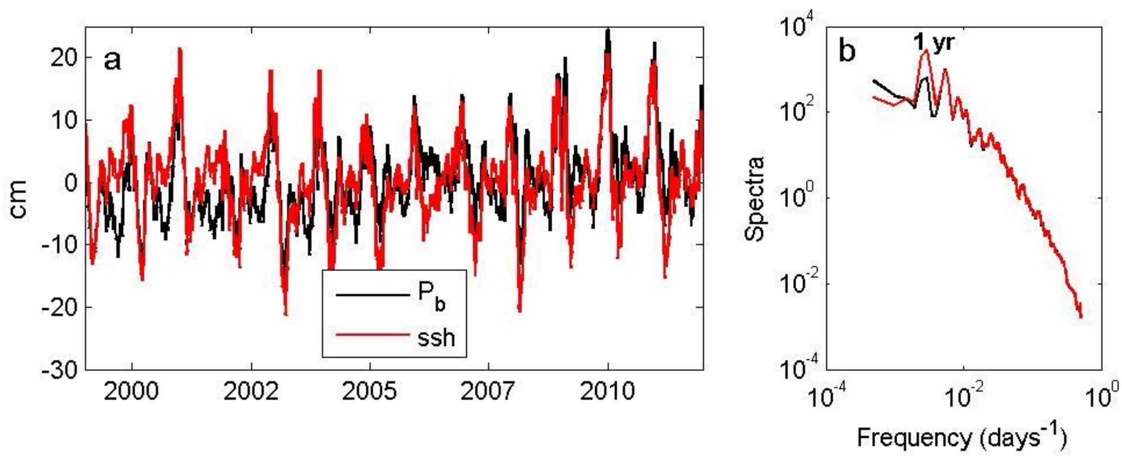

Figure 2. a) Basin average P_b (black) and ssh (red) and b) energy spectra of both curves.

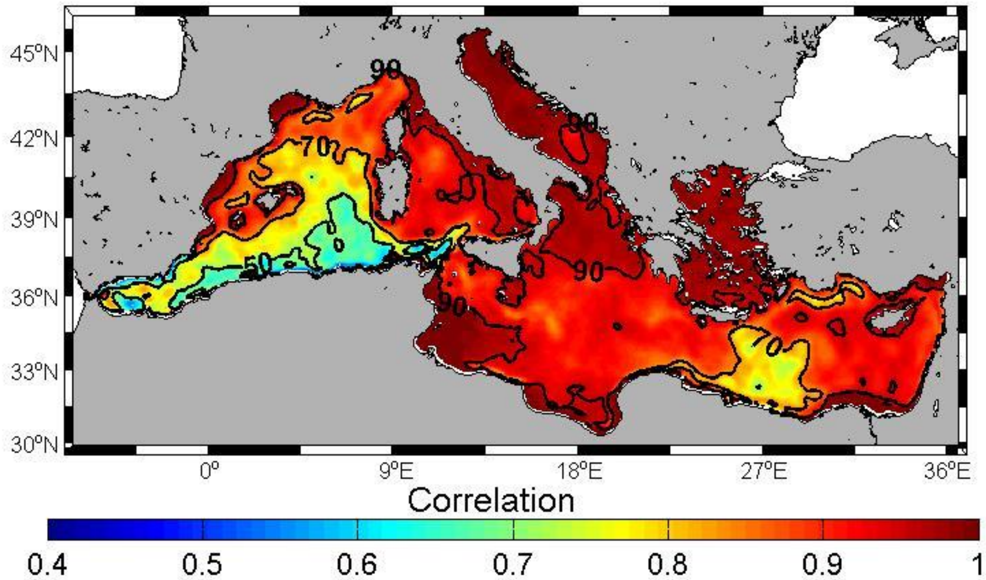

Figure 3. Correlation between high-passed filtered (<60days) P_b and sea level. Contour lines indicate percentage of variance of sea level explained by P_b.

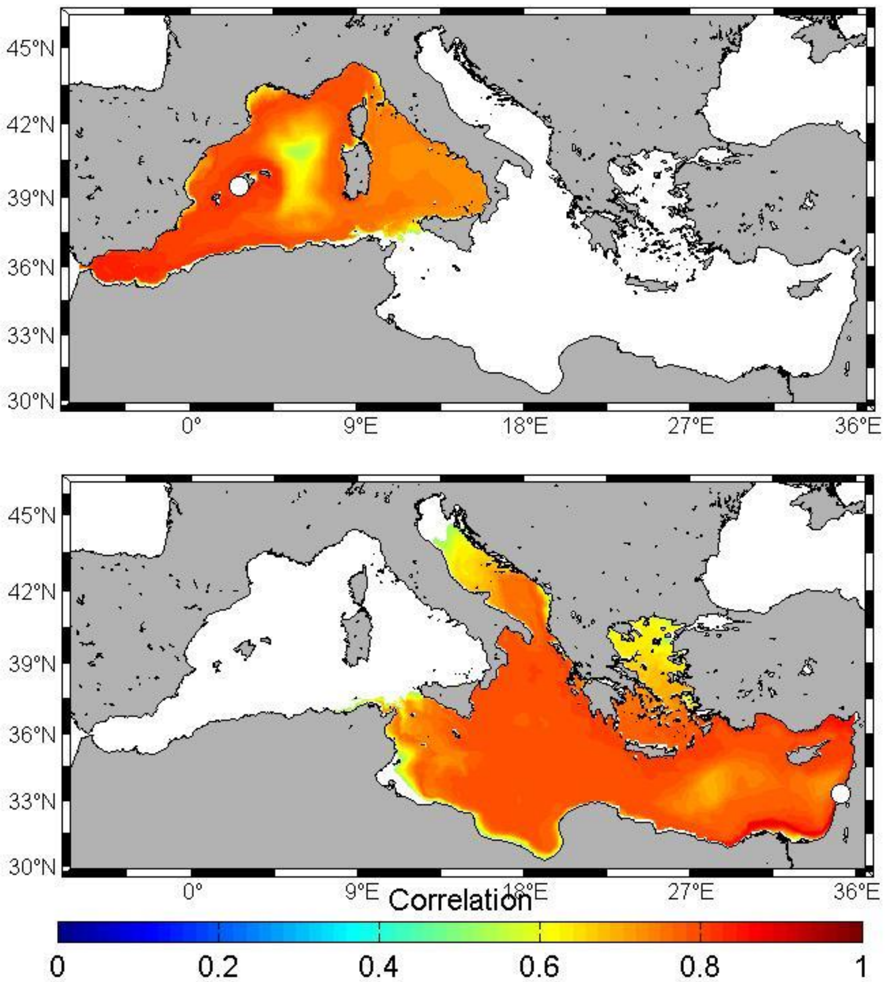

Figure 4. Correlation between high-passed (<60 days) filtered sea level at two points at the Levantine basin (bottom) and at Mallorca island (top) and P_b over the domain. Only areas where correlation is statistically significant at the 95% confidence level are shown. The locations of the points are indicated with a white dot.

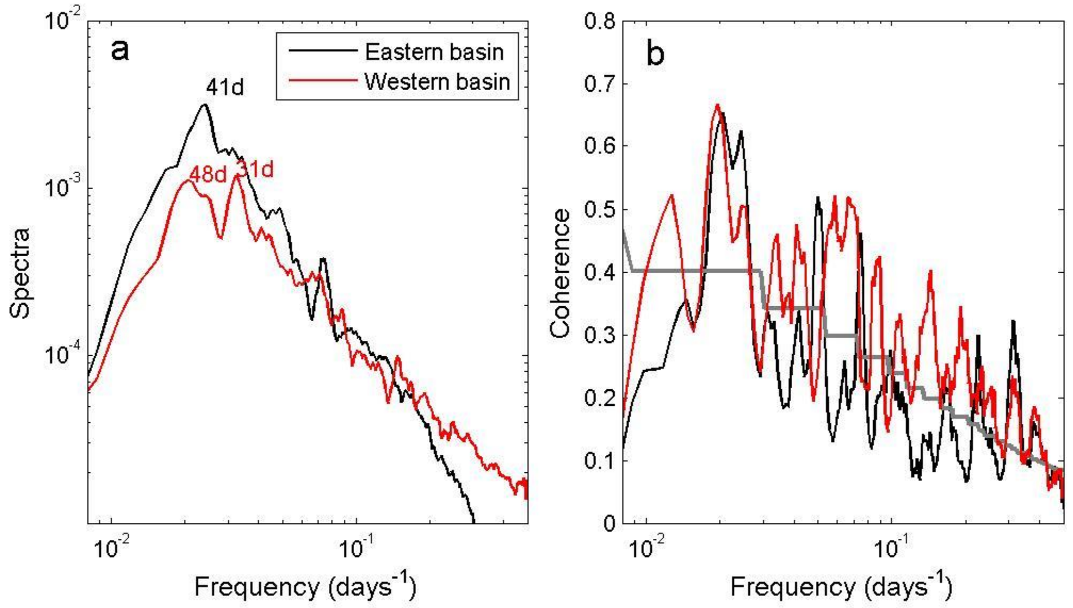

Figure 5. a) Power spectra of averaged high-passed filtered P_b on the eastern (black) and western (red) subbasins. Periods corresponding to major peaks are labelled. b) Coherence analyses between averaged high-passed filtered P_b and zonal wind stress at Gibraltar. 99% confidence intervals for each frequencies are represented by a grey line.

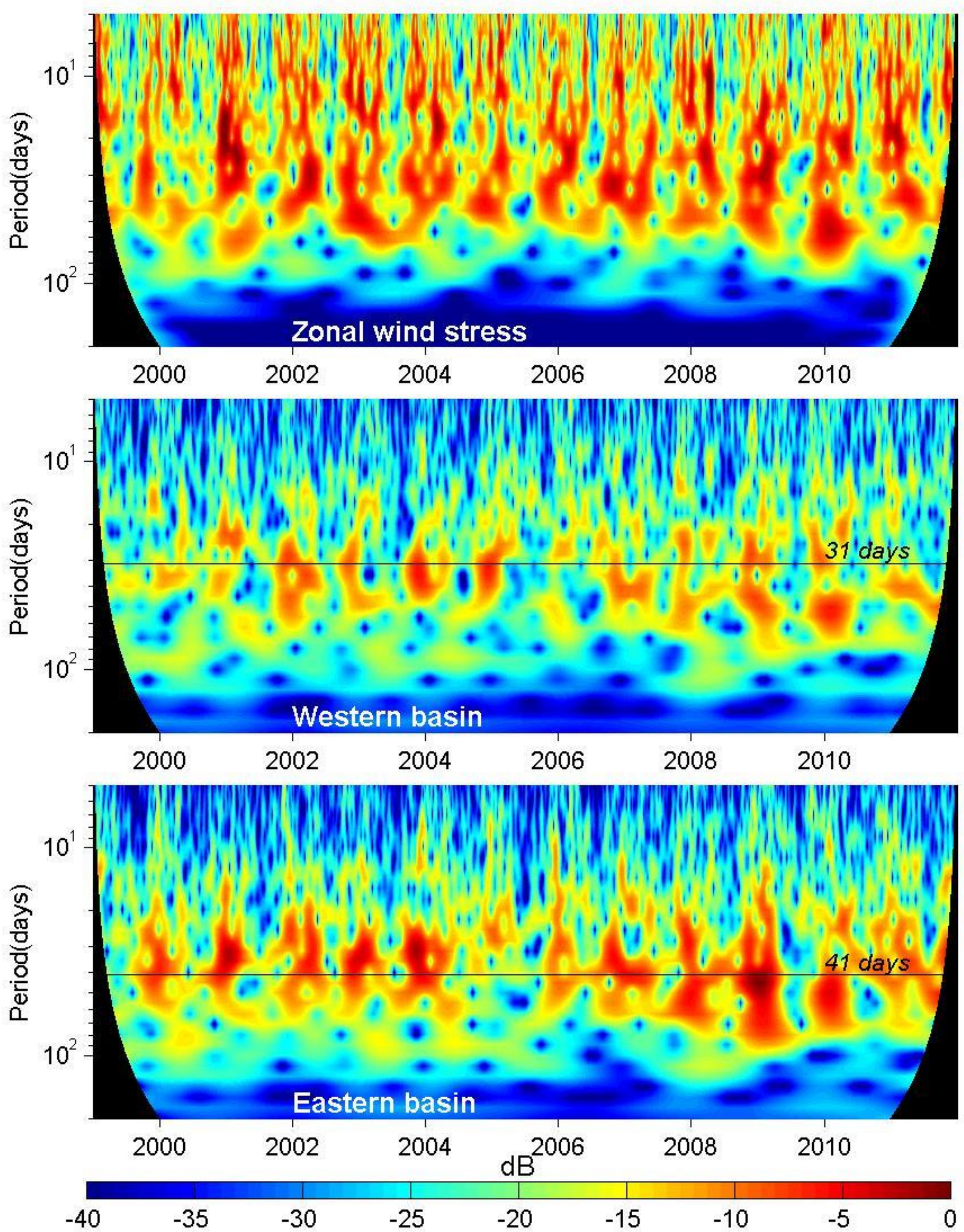

Figure 6. Wavelet analysis of zonal wind stress at Gibraltar (top) and averaged high-passed filtered P_b on the western (middle) and eastern (bottom) subbasins. Energy is normalized in dB.

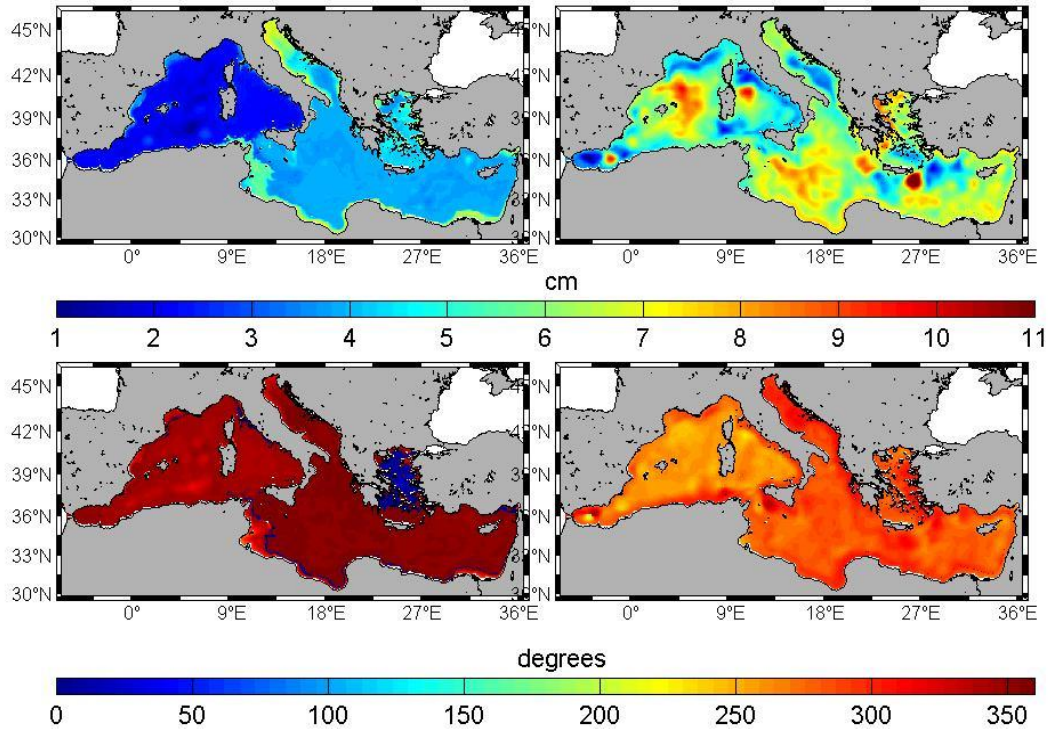

Figure 7. Annual amplitudes (top) and phases (bottom) of P_b (left) and sea level (right).

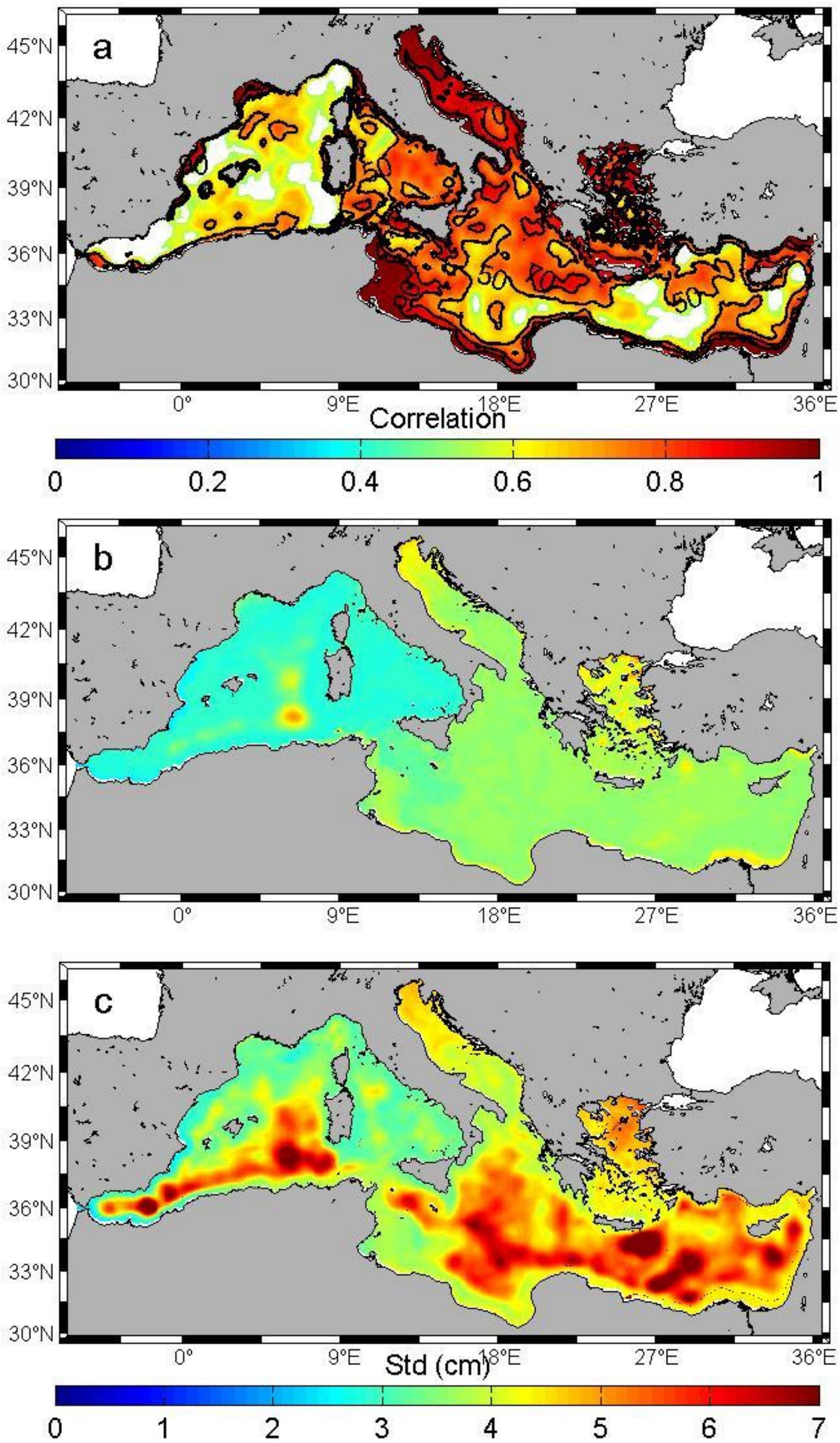

Figure 8. a)Correlation between low-passed filtered (> 60 days) and deseasoned P_b and sea level. Only areas where correlation is statistically significant at the 95% confidence level are shown. Contour lines indicate percentage of variance of sea level explained by

P_b. b) and c) Standard deviations of non-seasonal low-pass filtered P_b and sea level, respectively.

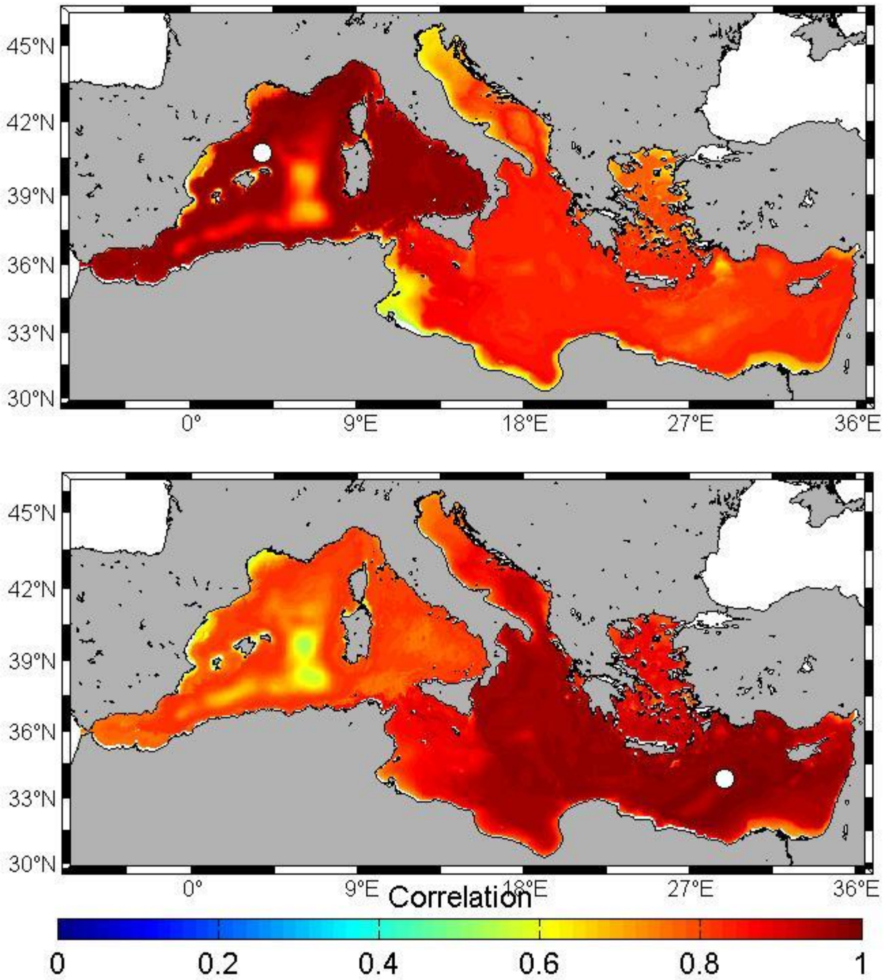

Figure 9: Correlation between low-passed filtered and deseasoned P_b at two deep ocean points at the eastern (bottom) and western (top) basins and P_b over the domain. The locations of the points are indicated with a white dot. Only areas where correlation is statistically significant at the 95% confidence level are shown.

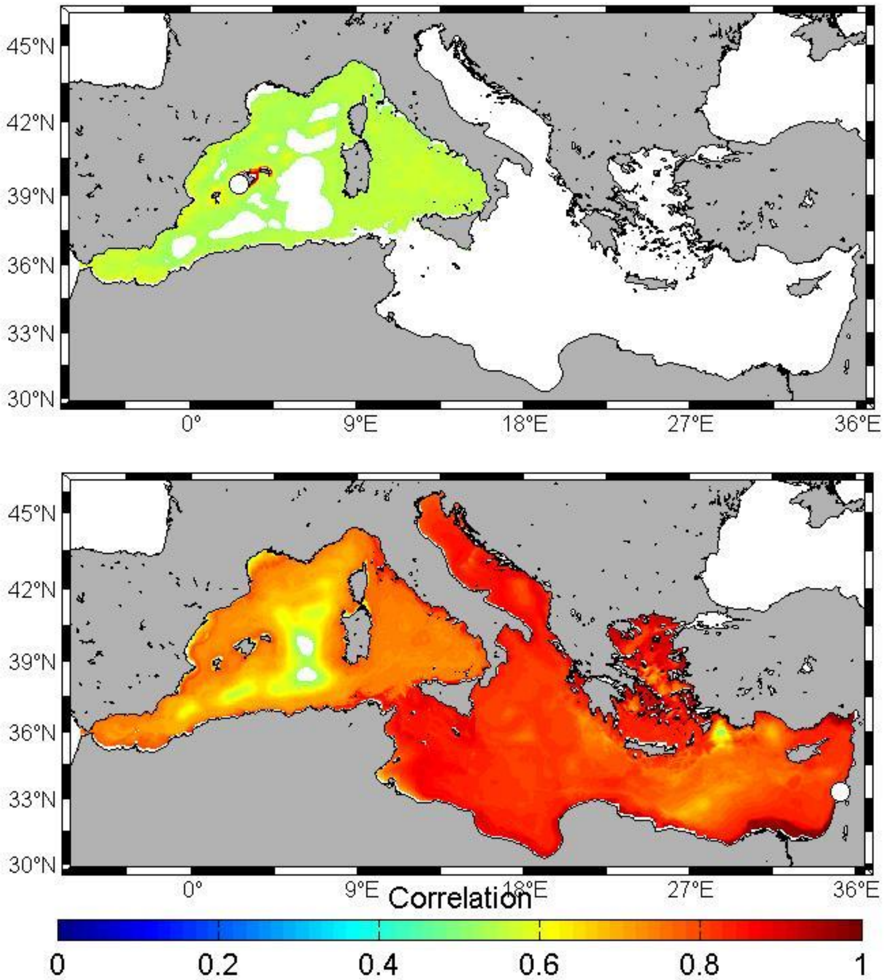

Figure 10: Correlation between low-passed filtered and deseasoned sea level at two points at the Levantine basin (bottom) and at Mallorca island (top) and P_b over the domain. The locations of the points are indicated with a white dot. Only areas where correlation is statistically significant at the 95% confidence level are shown.

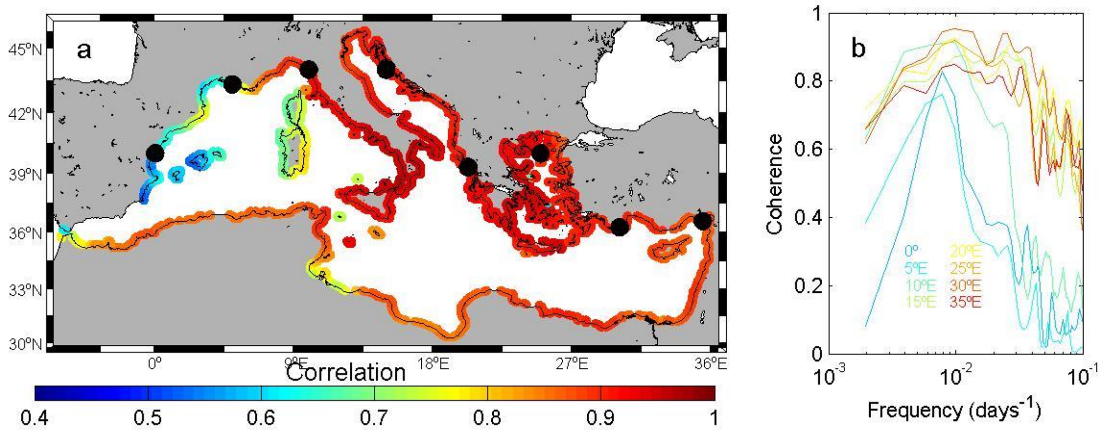

Figure 11. a) Correlations between coastal sea level and averaged P_b over the Mediterranean Sea. Time series are low-passed filtered with a cut-off period of 60 days and deseasoned. Only statistically significant at the 95% confidence level have been plotted. b) Coherence between coastal sea level and basin averaged P_b at selected points marked with black dots in (a).